

3. V. N. Nikolaevskii, K. S. Basniev, A. T. Gorbunov, and G. A. Zotov, The Mechanics of Saturated Porous Media [in Russian], Nedra, Moscow (1970).
4. R. I. Nigmatulin, Fundamentals of the Mechanics of Heterogeneous Media [in Russian], Nauka, Moscow (1978).
5. B. L. Rozhdestvenskii and N. N. Yanenko, Systems of Quasilinear Equations [in Russian], Nauka, Moscow (1968).
6. L. D. Landau and E. M. Livshits, The Mechanics of Solid Media [in Russian], Gostekhizdat, Moscow (1954).
7. N. A. Kudryashov and V. V. Murzenko, "Self-similar solution of problems involving axially symmetric gas flow through a porous medium with a quadratic resistance dependence," *Izv. Akad. Nauk SSSR, Mekh. Zhidk. Gaza*, No. 4 (1982).
8. A. G. Bondarenko, V. M. Kolabashkin, and N. A. Kudryashov, "Self-similar solution of problems involving gas flow through a porous medium under conditions of turbulent filtration," *Prikl. Mat. Mekh.*, 44, No. 3 (1980).
9. G. I. Barenblatt, "Self-similar flow of compressed liquid in a porous medium," *Prikl. Mat. Mekh.*, 16, No. 6 (1952).
10. V. M. Kovenya and N. N. Yanenko, The Method of Decomposition in Problems of Gasdynamics [in Russian], Nauka, Novosibirsk (1981).
11. J. P. Boris and D. L. Book, "Solving equations of discontinuity by the method of flux corrections," in: Calculation Methods in the Physics of Plasma [Russian translation], J. Killen (ed.), Mir, Moscow (1980).
12. J. P. Boris and D. L. Book, "Fully multidimensional flux-corrected transport algorithms for fluids," *J. Comput. Phys.*, 11, No. 38 (1979).

INFLUENCE OF THE SHOCK LAYER ON THE VISCOUS DRAG  
OF STAR-SHAPED BODIES WITH PLANAR SIDE PANELS

G. I. Shchepanovskaya and V. A. Shchepanovskii

UDC 533.6.013.12

The ratio of the wave drag determined by the intensity of the corresponding shock layer and the viscous drag due to surface friction is practically clear for three-dimensional bodies of concave cross section, but for star-shaped configurations some further development is necessary. Calculations using linear theory [1], from which we see that the wave drag of a star-shaped body is less than that of a body of revolution of equivalent length and volume, only serve to stress the desirability of such a study.

For a fixed length of a configuration with planar side panels the wave drag is determined by the relative thickness, and depends slightly on the number of petals [2, 3]. As the thickness decreases, for unchanged body length and number of petals, and for a fixed volume, the wave drag decreases, the viscous drag increases, and the size of the petals increases, leading to a considerable increase of the washed surface area [4]. The external inviscid flow for the boundary layer on the configuration surface is the flow behind the bow shock wave (the shock layer). In calculating the viscous drag coefficient one must consider each petal as a flat plate with a skewed leading edge [2, 5, 6]. The friction drag is determined by integrating the local coefficient over the surface.

In this paper we investigate the influence of the shock layer on the boundary layer characteristics and the friction drag. We calculate the friction coefficient as a function of the incident stream parameters and the shape geometry. The wave and viscous drag coefficients are compared.

1. We consider supersonic flow over a star-shaped body, with uniform flow over the planar side panels. The unperturbed flow velocity  $U_\infty$  is directed along the body axis. The shape geometry is fully determined by giving the linear size  $D$  (the diameter of the cone of equivalent length and volume) and three dimensionless parameters:  $\lambda$ , the elongation (ratio of the

---

Krasnoyarsk. Translated from *Zhurnal Prikladnoi Mekhaniki i Tekhnicheskoi Fiziki*, No. 4, pp. 105-112, July-August, 1985. Original article submitted June 14, 1984.

length  $L$  of the star to  $D$ );  $r$ , the ratio of the diameter of the circle inscribed in the midsection to  $D$ ; and  $n$ , an integer parameter giving the number of petals. It follows from the definition of the parameters that  $r < 1$ , while the quantity  $\xi = r/(2\lambda)$  describes the relative thickness of the configuration.

An individual petal of the star is a three-dimensional analog of a planar wedge, from the viewpoint of gasdynamic structure [7]. Then the pressure on the washed surface for a given Mach number  $M_\infty$  is given by the relation [8]

$$\frac{p_1}{\frac{1}{2} \rho_\infty U_\infty^2} = \frac{2\xi}{\xi + \zeta} + \frac{2}{\kappa M_\infty^2} \quad (1.1)$$

where  $\kappa$  is the adiabatic index, and  $\zeta$  is a root of the equation

$$\zeta^3 + \xi \left(1 + \frac{\kappa+1}{2} M_\infty^2\right) \zeta^2 + (1 - M_\infty^2) \zeta + \xi \left(1 + \frac{\kappa-1}{2} M_\infty^2\right) = 0.$$

In accordance with this model we can find the distributions of density, temperature, and velocity in the shock layer:

$$\frac{\rho_1}{\rho_\infty} = \frac{\xi + \zeta}{\zeta(1 - \xi\zeta)} \quad (1.2)$$

$$\frac{T_1}{T_\infty} = \frac{[2\kappa M_\infty^2 - (\kappa-1)(1 + \zeta^2)] [(\kappa-1)M_\infty^2 + 2(1 + \zeta^2)]}{(\kappa+1)^2 (1 + \zeta^2) M_\infty^2} \quad (1.3)$$

$$\frac{M_1}{M_\infty} = \frac{\zeta \sqrt{1 + \xi^2}}{\xi + \zeta} \sqrt{\frac{T_\infty}{T_1}} \quad (1.4)$$

where quantities with the subscript  $\infty$  refer to the corresponding parameters of the unperturbed flow.

The wave drag of the configuration, taking account of Eq. (1.1), has the form

$$c_w = \frac{X_w}{\frac{1}{2} \rho_\infty U_\infty^2 S_M} = \frac{2}{\kappa M_\infty^2} + \frac{2\xi}{\xi + \zeta} \quad (1.5)$$

which is determined only by the thickness  $\xi = r/(2\lambda)$  and does not depend on the number of rays ( $S_M$  is the area of the base of the configuration). In calculating the wave drag in Eq. (1.5) we assume a vacuum at the edge of the base.

This approximate model describing the viscous flow of Eqs. (1.1)-(1.4) gives an exact solution, allowing for the nonlinear interactions of [8] for the Mach number of the incident flow:

$$M_\infty^2 = \frac{(1 + 4\lambda^2\varphi)(1 + 4r^2\lambda^2\varphi^2)}{4\lambda^2\varphi \left(1 - \frac{\kappa+1}{2} r^2\varphi\right) - \frac{\kappa-1}{2}}, \quad \varphi = \frac{n}{\pi} \operatorname{tg} \frac{\pi}{n}. \quad (1.6)$$

Equation (1.6) gives a supersonic incident stream for

$$r^2 < 2/[(\kappa+1)\varphi], \quad \lambda^2 > (\kappa-1) / \left[8\varphi \left(1 - \frac{\kappa+1}{2} r^2\varphi\right)\right].$$

Taking account of the dependence of  $\varphi$  on the number of petals, we obtain the conditions for the existence of Eq. (1.6), independent of  $n$ :

$$r^2 < \frac{2}{(\kappa+1)\varphi(3)^{\frac{1}{2}}}, \quad \lambda^2 > \frac{\kappa-1}{8 \left[1 - \frac{\kappa+1}{2} r^2\varphi(3)\right]}. \quad (1.7)$$

2. The friction drag of the wetted surface of a star-shaped body with planar side panels can be calculated on the assumption that each side panel ABC (Fig. 1) is washed like a plate with a skewed leading edge by a supersonic stream with velocity  $U_1$  of Eq. (1.4) in the direction of the internal rib CB. The distribution of the gasdynamic quantities at the boundary layer edge is determined from the inviscid flow of Eqs. (1.1)-(1.4).

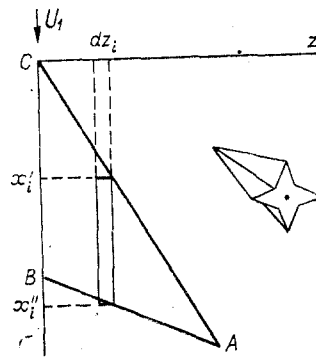


Fig. 1

The panel of the petal ABC is divided into elementary bands of width  $dz_i$  (see Fig. 1). If there is no interaction of the flows between bands the laminar boundary layer of the  $i$ -th band is given by the equations

$$\begin{aligned} \rho \left( u \frac{\partial u}{\partial x} + v \frac{\partial u}{\partial y} \right) &= -\frac{dp_1}{dx} + \frac{\partial}{\partial y} \left( \mu \frac{\partial u}{\partial y} \right), \quad \frac{\partial(\rho u)}{\partial x} + \frac{\partial(\rho v)}{\partial y} = 0, \\ \rho \left( u \frac{\partial \Theta}{\partial x} + v \frac{\partial \Theta}{\partial y} \right) &= \frac{1}{Pr} \frac{\partial}{\partial y} \left( \mu \frac{\partial \Theta}{\partial y} \right) + \frac{\kappa-1}{\kappa} \left( 1 - \frac{1}{Pr} \right) \frac{\partial}{\partial y} \left( \frac{\mu u}{R} \frac{\partial u}{\partial y} \right), \\ \Theta &= T + \frac{\kappa-1}{\kappa} \frac{u^2}{R}, \quad p_1 = \rho RT, \quad \mu = \mu_0 (T/T_0)^m, \end{aligned}$$

where  $u$  and  $v$  are the components of the velocity vector on the axes  $x$  and  $y$ , respectively; the  $y$  axis is directed perpendicular to the plane of the panel  $x, z$ ;  $\mu$  is the dynamic viscosity; and  $\mu_0 T_0$  are the corresponding parameters of the adiabatically stagnated flow. The Prandtl number is determined from the specific heat  $c_p$  and the thermal conductivity  $\sigma$ :  $Pr = \mu c_p / \sigma$ .

The boundary conditions for velocity and temperature on the washed surface, on the assumption that the panel is thermally insulated, have the form  $u = v = 0$ ,  $\partial T / \partial y = 0$ , and  $u = U_1$ ,  $T = T_1$  at an infinite distance from the surface. The quantities with subscript 1 are found by solving the inviscid problem of Eqs. (1.1)-(1.4).

The solution of this problem is well known [9] for Prandtl number equal to 1. The friction stress as a function of the coordinate  $x$  of the  $i$ -th band is determined by the relation

$$\tau_w(x) = \left( \mu \frac{\partial u}{\partial y} \right)_w = \frac{1}{2} \rho_1 U_1^2 A_{12} \frac{1}{\sqrt{Re_x}} \quad (2.1)$$

where  $A_{12} = 0.664 \left( 1 + \frac{\kappa-1}{2} M_1^2 \right)^{\frac{m-1}{2}}$ ;  $Re_x = \frac{\rho_1 U_1}{\mu_1} (x - x_i')$ ;  $x_i'$  is the abscissa of the start of the  $i$ -th band; and  $x \geq x_i'$ .

For a turbulent boundary layer, following the results of [10], we can write the friction stress of the  $i$ -th band in the form

$$\tau_w(x) = \frac{1}{2} \rho_1 U_1^2 A_{15} Re_x^{-\frac{1}{5}} \quad (2.2)$$

Subsequently, expressions (2.1) and (2.2) are considered simultaneously:

$$\tau_w(x) = \frac{1}{2} \rho_1 U_1^2 A_{1k} Re_x^{-1/k} \quad (2.3)$$

( $k = 2$  corresponds to laminar flow, and  $k = 5$  corresponds to turbulent flow).

The length of the  $i$ -th band is given by the quantity  $x_i'' - x_i'$ , where  $x_i'$  and  $x_i''$  are, respectively, the coordinates of the start and end of the band. If we introduce the quantities  $S_{\Delta} = \bar{S}_{\Delta} D^2$  [the area of the triangle ABC (see Fig. 1)] and  $a = aD = D\lambda\sqrt{1 + \xi^2}$  [the length of the side BC (the internal rib of the configuration)], then for the length of the  $i$ -th band we obtain the expression

$$l_i = x_i'' - x_i' = \left( \frac{2S_\Delta}{a} - z_i \right) \frac{a^2}{2S_\Delta}. \quad (2.4)$$

The friction drag of the  $i$ -th band is obtained by integrating Eq. (2.3) over the length

$$X_F^i = dz_i \frac{1}{2} \rho_1 U_1^2 A_{1k} \left( \frac{\rho_1 U_1}{\mu_1} \right)^{-\frac{1}{k}} \int_{x_i'}^{x_i''} (x - x_i')^{-\frac{1}{k}} dx.$$

Allowing for Eq. (2.4) we have

$$X_F^i = \frac{1}{2} \rho_1 U_1^2 A_{1k} \left( \frac{\rho_1 U_1}{\mu_1} \right)^{-\frac{1}{k}} \frac{1}{1 - \frac{1}{k}} \left[ \frac{a^2}{2S_\Delta} \left( \frac{2S_\Delta}{a} - z_i \right) \right]^{1 - \frac{1}{k}} dz_i.$$

By integration over  $z$  we find the viscous drag of the entire surface of the triangular panel ABC:

$$\begin{aligned} X_F &= \frac{1}{2} \rho_1 U_1^2 A_{1k} \left( \frac{\rho_1 U_1}{\mu_1} \right)^{-\frac{1}{k}} \left( \frac{a^2}{2S_\Delta} \right)^{1 - \frac{1}{k}} \frac{1}{1 - \frac{1}{k}} \int_0^{\frac{2S_\Delta}{a}} \left( \frac{2S_\Delta}{a} - z \right)^{1 - \frac{1}{k}} dz = \\ &= \frac{1}{2} \rho_1 U_1^2 A_{1k} \left( \frac{\rho_1 U_1}{\mu_1} \right)^{-\frac{1}{k}} \left( \frac{a^2}{2S_\Delta} \right)^{1 - \frac{1}{k}} \frac{1}{1 - \frac{1}{k}} \frac{1}{2 - \frac{1}{k}} \left( \frac{2S_\Delta}{a} \right)^{2 - \frac{1}{k}} = \\ &= \frac{1}{2} \rho_1 U_1^2 A_{1k} [1 + \xi^2]^{-\frac{1}{2k}} \lambda^{-\frac{1}{k}} \frac{2k^2 S_\Delta}{(2k-1)(k-1)} \left( \frac{\rho_1 U_1 D}{\mu_1} \right)^{-\frac{1}{k}}. \end{aligned}$$

The side surface of the entire configuration consists of  $2n$  identical triangles ABC and is  $S_* = 2nS_\Delta$ . For the viscous drag coefficient we find

$$c_F = \frac{2nX_F}{\frac{1}{2} \rho_\infty U_\infty^2 S_M} = \frac{\rho_1 U_1^2}{\rho_\infty U_\infty^2} \left( \frac{\rho_1 U_1 \mu_\infty}{\rho_\infty U_\infty \mu_1} \right)^{-\frac{1}{k}} \lambda^{-\frac{1}{k}} (1 + \xi^2)^{-\frac{1}{2k}} \frac{2k^2}{(2k-1)(k-1)} \frac{S_*}{S_M} A_{1k} \left( \frac{\rho_\infty U_\infty D}{\mu_\infty} \right)^{-\frac{1}{k}}.$$

Using expressions for the gasdynamic quantities in the shock layer, Eqs. (1.2)-(1.4), and taking account of the relation between the speed of sound and the temperature  $(c_1/c_\infty) = \sqrt{T_1/T_\infty}$ , we finally obtain for the viscous drag coefficient

$$\begin{aligned} c_F &= A_{1k} A_{2k} \lambda^{-\frac{1}{k}} (1 + \xi^2)^{-\frac{1}{2k}} \frac{2k^2}{(2k-1)(k-1)} \frac{S_*}{S_M} \text{Re} \frac{1}{D_*} \\ A_{2k} &= \left( \frac{\rho_1}{\rho_\infty} \right)^{\frac{k-1}{k}} \left( \frac{M_1}{M_\infty} \right)^{\frac{2k-1}{k}} \left( \frac{T_1}{T_\infty} \right)^{\frac{2(k+m)-1}{2k}} \end{aligned} \quad (2.5)$$

where  $\text{Re}D = \rho_\infty U_\infty D / \mu_\infty$  is the Reynolds number based on the parameters of the unperturbed flow; as the linear dimension we take the diameter of the equivalent cone. Conversion in Eq. (2.5) to Reynolds number based on the configuration length  $L$  is effected by means of the formula  $\text{Re}_L = \lambda \text{Re}D$ .

The coefficient  $A_{1k}$  refers to the viscous solution of Eq. (2.3) and accounts for the compressibility of flow in the boundary layer, and the coefficient  $A_{2k}$  accounts for the influence of the shock layer. For the laminar boundary layer  $k = 2$  and Table 1 shows numerical values of the coefficients as a function of the incident stream Mach number for the configurations  $\lambda = 2$ ,  $r = 0.5$ ,  $n = 4$ ,  $\kappa = 1.4$ ,  $m = 0.76$ ,  $\text{Re}D = 6.5 \cdot 10^4$ ,  $M_1$  is the Mach number for the flow

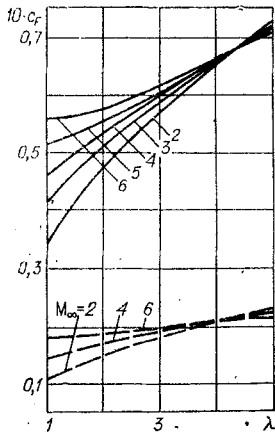


Fig. 2

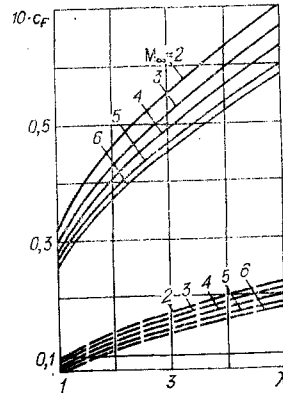


Fig. 3

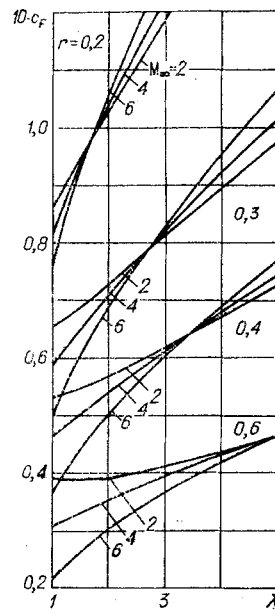


Fig. 4

TABLE 1

$M_\infty$	$M_1$	$A_\infty$	$A_{12}$	$A_{22}$	$A_{12}A_{22}$
2	1,74	0,61877	0,62721	1,06112	0,66554
3	2,64	0,58682	0,59791	1,18637	0,70934
4	3,48	0,55895	0,57276	1,29458	0,74148
5	4,27	0,53553	0,55215	1,39908	0,77250
6	5,02	0,51583	0,53512	1,50380	0,80471

in the boundary layer of Eq. (1.4). The quantity  $A_\infty = A_{12}A_{22} = 0.664 \left(1 + \frac{\kappa-1}{2} M_\infty^2\right)^{(m-1)/2}$  describes a corrected coefficient in Eq. (2.5) when there is no shock layer, i.e., the external flow for the boundary layer coincides with the unperturbed stream. In this case,  $M_1 = M_\infty$ ,  $A_{22} = 1$ .

3. Figures 2-6 show calculated drag of star-shaped configurations for laminar flow in the boundary layer,  $k = 2$ , as a function of the geometry parameters and the flow conditions. In the calculations we assumed  $\kappa = 1.4$ ,  $m = 0.76$ .

Figure 2 shows the calculated viscous drag coefficient from Eq. (2.5) for a star-shaped configuration with  $r = 0.5$  and four petals, as a function of the shape elongation  $\lambda$  and the incident stream Mach number. The solid lines correspond to Reynolds number  $Re_D = 6.5 \cdot 10^4$ , and the broken lines to  $Re_D = 6.5 \cdot 10^5$ . With increase of  $\lambda$  the friction drag increases, since there is an increase in the relative wetted surface. The dependence of the friction drag on the incident stream Mach number is more complex. Up to a certain value of  $\lambda$  the friction drag increases with increase in the Mach number, but the opposite is true for more elongated configurations: A smaller viscous drag coefficient, as in Eq. (2.5), corresponds to a larger incident stream Mach number.

Figure 3 shows the results of an analogous calculation for the same values, but without accounting for the influence of the shock layer on the formation of the viscous flow, i.e.,  $A_{22} = 1$ . It can be seen that the qualitative dependence of  $c_F$  on  $M_\infty$  is the same as in Fig. 2 for the larger elongations ( $\lambda \gg 1$ ). Consequently, the dependence of the viscous drag on incident stream Mach number in Fig. 2 is due to the influence of nonlinear processes on flow formation in the shock layer behind the bow shock. For the larger elongation values ( $\lambda \gg 1$ ) the relative configuration thickness  $\xi = r/2\lambda$  is small and the flow in the shock layer, Eqs. (1.2)-(1.4) (the external flow for the boundary layer) differs insignificantly from the incident stream, the quantity  $A_{22} \approx 1$  and the qualitative dependence of  $c_F$  on  $M_\infty$  for large  $\lambda$  (see Fig. 2) is the same as in Fig. 3.

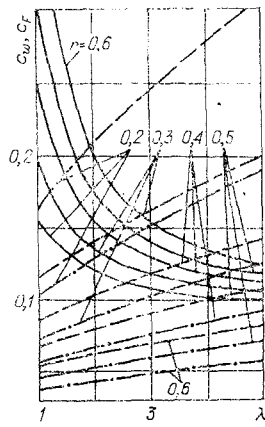


Fig. 5

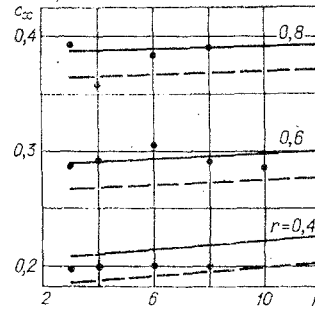


Fig. 6

Figures 4-6 show the calculated flow, allowing for the shock layer  $A_{22} \neq 1$ , for laminar boundary layer conditions. Figure 4 shows the dependence of  $c_f$  on the geometry parameters  $r$  and  $\lambda$  for four-petal configurations with  $Re_D = 10^5$  and incident stream Mach numbers of 2, 4, and 6. For a fixed elongation  $\lambda$  the viscous drag increases with decrease of  $r$ , since when the configuration volume is held constant the petal size is large for small  $r$ , and, therefore, the wetted surface  $S_x$  is large. The value of elongation  $\lambda$  for which there is a change in the qualitative dependence of the viscous friction drag on the Mach number is displaced toward smaller  $\lambda$  with decrease of  $r$ . The intensity of the shock layer in Eqs. (1.1)-(1.4) is determined by the value of  $\xi$ . It can be seen from the calculations in Figs. 2 and 4 that there is a change in the qualitative dependence of  $c_f$  on  $M_\infty$  for  $\xi \approx 0.06$ ; therefore, for thin configurations with  $\xi \leq 0.05$  we can neglect the influence of the shock layer on the viscous flow, i.e., put  $M_1 = M_\infty$  and  $A_{2k} = 1$  in Eq. (2.5).

Figure 5 shows a comparison of the wave drag, Eq. (1.5), and the friction drag, Eq. (2.5) for  $Re_D = 6.5 \cdot 10^4$  and  $M_\infty = 4$ . The coefficients are given on a single scale. The solid lines show wave drag curves for  $r = 0.2-0.6$  as a function of the elongation. The broken lines show the calculated viscous drag for configurations with number of petals  $n = 7$ , and the dot-dash lines show the same thing for  $n = 4$ . As follows from Eq. (1.5), the wave drag does not depend on  $n$ , and the conditions at the outer edge of the boundary layer are the same for  $n = 4$  and 7. The difference in the viscous drag coefficients for  $n = 4$  and 7 is determined by the area of the wetted surface, which is proportional to  $n$ . With decrease of  $r$  the viscous drag contribution becomes significant, even for four cycles. This contribution increases with increase of the configuration elongation  $\lambda$ , and for  $\lambda \geq 3$  the viscous and wave drag values are on the same order. With increase of  $r$  the wave drag has the opposite tendency, since the relative thickness  $\xi = r/2\lambda$  decreases.

Figure 6 shows the wave drag  $c_x = c_w + c_f$  (solid lines), where  $c_w$  and  $c_f$  are calculated from Eqs. (1.5) and (2.5), respectively, as a function of the number of cycles an elongation of  $\lambda = 1.3$  and incident flow parameters  $M_\infty = 4$ ,  $Re_D = 2.7 \cdot 10^6$ . The total drag depends slightly on the number  $n$ , since for  $\lambda = 1.3$  the main contribution is the wave drag, Eq. (1.5), which does not depend on  $n$ . However, for  $r = 0.4$ , this dependence on  $n$  is noticeable because of the value of  $c_f$ , Eq. (2.5).

The points on Fig. 6 show the experimental values of  $c_x$ , from [2]. For  $r = 0.6$  and 0.8 there is satisfactory agreement between the calculated and experimental values. For  $r = 0.4$  the theory overestimates the total drag by about 5%. The base pressure was assumed to be zero in the calculation (solid lines). The broken lines in Fig. 6 show the values of total drag, allowing for the base pressure in analogy with [11], which gives a correction of  $\Delta c_x = -0.022$  for the configurations examined. The experimental points lie above the broken lines, in a band whose width decreases with increase of the incident stream Mach number  $M_\infty$ .

We note that the configurations examined satisfy the conditions (1.7) and, therefore, Eq. (1.6) is satisfied. The approximate model for calculating the shock layer, Eqs. (1.1)-(1.4), and the boundary layer, Eq. (2.1), will give an exact solution for the incident stream Mach number, Eq. (1.6). In particular, for  $r = 0.6$  and  $\lambda = 1.3$ , this Mach number is 3.6. In Fig. 6 the calculation was made for  $M_\infty = 4.0$ , i.e., the values for  $r = 0.6$  are close to exact.

The elongated configurations with  $\xi \leq 0.05$  ( $\lambda > 5$ ,  $r < 0.5$ ) the influence of the shock layer on the viscous drag is insignificant, and it can be calculated from the unperturbed flow at the outer edge of the boundary layer [4]. For  $\lambda < 5$  and  $r > 0.3$ , the main contribution to the total drag comes from the wave drag, although even for  $2 \leq \lambda \leq 5$  and  $0.2 \leq r \leq 0.5$  the viscous drag can be on the same order.

The authors thank V. G. Dulov for his interest in the work and for discussions.

#### LITERATURE CITED

1. M. I. Folle, "The wave drag of elongated star-shaped bodies at moderate supersonic flight speed," *Izv. Akad. Nauk SSSR, Mekh. Zhidk. Gaza*, No. 5 (1983).
2. Yu. A. Vedernikov, A. L. Gonor, et al., "Aerodynamic characteristics of star-shaped bodies at Mach numbers  $M = 3-5$ ," *Izv. Akad. Nauk SSSR, Mekh. Zhidk. Gaza*, No. 4 (1981).
3. M. A. Zubin, V. I. Lapygin, and N. A. Astananko, "Theoretical and experimental investigation of the structure of supersonic flow over star-shaped bodies and their aerodynamic characteristics," *Izv. Akad. Nauk SSSR, Mekh. Zhidk. Gaza*, No. 3 (1982).
4. V. A. Bordyug and G. I. Shchepanovskaya, "The influence of elongation and number of petals of a star-shaped configuration on the drag in supersonic flow," in: Part I of the All-Union Seminar School on Multidimensional Problems of Mechanics of Continuous Media, Krasnoyarsk (1983) (Deposited 8/25/1983; No. 4623-83 Dep.).
5. G. I. Maikapar and A. I. Pyatnova, "The drag of a wedge with disks at supersonic speeds," *Uchen. Zap. Tsentr. Aero. Hidro. Inst.*, Vol. 12, No. 4 (1981).
6. V. A. Bordyug and G. I. Shchepanovskaya, *The Viscous Drag of Star-Shaped Bodies in Supersonic Flow* [in Russian], Preprint, Vychisl. Tsentr. Sib. Otd. Akad. Nauk SSSR, No. 3, Krasnoyarsk (1983).
7. V. A. Shchepanovskii, "Specification of the gasdynamic structure of star-shaped configurations," in: Part I of the All-Union School Seminar on Multidimensional Problems of Mechanics of Continuous Media [in Russian], Krasnoyarsk (1983) (Deposited 8/25/1983; No. 4623-83 Dep.).
8. V. A. Bodyug, Yu. A. Vedernikov, et al., "Parametric investigation of hypersonic three-dimensional shapes," *Zh. Prikl. Mekh. Tekh. Fiz.*, No. 1 (1983).
9. N. E. Kochin, I. A. Kibel, and N. V. Roze, *Theoretical Hydromechanics* [in Russian], Part II, Fizmatgiz, Moscow (1963).
10. V. M. Garbuzov, N. P. Kolina, and A. I. Pyatnova, "Calculation of the Coefficients of Friction Drag and Heat Transfer of a Plate and a Sharp Cone, Washed by a Supersonic Stream, with Turbulent Flow in the Boundary Layer" [in Russian], *Tr. Tsentr. Aero. Hidro. Inst.*, No. 1881 (1977).
11. G. I. Maikapar and A. I. Pyatnova, "Choice of the Main Parameters of a Wing of  $\Lambda$ -Shaped Cross Section" [in Russian], *Uchen. Zap. Tsentr. Aero. Hidro. Inst.*, Vol. 15, No. 1 (1984).